

## Article

# Remote Sensing Based Estimation of Evapo-Transpiration Using Selected Algorithms: The Case of Wonji Shoa Sugar Cane Estate, Ethiopia

Mulugeta Genanu <sup>1,\*</sup>, Tena Alamirew <sup>2</sup>, Gabriel Senay <sup>3</sup> and Mekonnen Gebremichael <sup>4</sup>

<sup>1</sup> College of Natural Sciences Arba Minch University, Arba Minch P.O. Box 21, Ethiopia

<sup>2</sup> Water and Land Resource Centre, Addis Ababa University, Addis Ababa P.O. Box 1176, Ethiopia, tena.a@wlrc-eth.org

<sup>3</sup> USGS Earth Resources Observation and Science (EROS) Center, Sioux Falls, SD 57198-0001, USA, senay@usgs.gov

<sup>4</sup> Civil and Environmental Engineering Department, University of California, Los Angeles, Los Angeles, CA 90095, USA, mekonnen@engr.uconn.edu

\* Correspondence: mule.genanu@gmail.com

**Abstract:** Remote sensing datasets are increasingly being used to provide spatially explicit large scale evapotranspiration (ET) estimates. The focus of this study was to estimate and thematically map pixel-by-pixel basis, and compare the actual evapotranspiration (ETa) of the Wonji Shoa Sugarcane Estate using Surface Energy Balance Algorithm for Land (SEBAL), Simplified Surface Energy Balance (SSEB) and Operational Simplified Surface Energy Balance (SSEBop) algorithms on Landsat7 ETM+ images acquired on four days in 2002. The algorithms were based on image processing which uses spatially distributed spectral satellite data and ground meteorological data to derive the surface energy balance components. The results obtained revealed that the ranges of the daily ETa estimated on January 25, February 26, September 06 and October 08, 2002 using SEBAL were 0.0–6.85, 0.0–9.36, 0.0–3.61, 0.0–6.83 mm/day; using SSEB 0.0–6.78, 0.0–7.81, 0.0–3.65, 0.0–6.46 mm/day, and SSEBop were 0.05–8.25, 0.0–8.82, 0.2–4.0, 0.0–7.40 mm/day, respectively. The Root Mean Square Error (RMSE) values between SSEB and SEBAL, SSEBop and SEBAL, and SSEB and SSEBop were 0.548, 0.548, and 0.99 for January 25, 2002; 0.739, 0.753, and 0.994 for February 26, 2002; 0.847, 0.846, and 0.999 for September 06, 2002; 0.573, 0.573, and 1.00 for October 08, 2002, respectively. The standard deviation of ETa over the sugarcane estate showed high spatio-temporal variability perhaps due to soil moisture variability and surface cover. The three algorithm results showed that well watered sugarcane fields in the mid-season growing stage of the crop and water storage areas had higher ETa values compared with the other dry agricultural fields confirming that they consumptively use more water. Generally during the dry season ETa is limited to water surplus areas only and in wet season, ETa was high throughout the entire sugarcane estate. The evaporation fraction (ETrF) results also followed the same pattern as the daily ETa over the sugarcane estate. The total crop and irrigation water requirement and effective rainfall estimated using the Cropwat model were 2468.8, 2061.6 and 423.8 mm/yr for January 2001 planted and 2281.9, 1851.0 and 437.8 mm/yr for March 2001 planted sugarcane, respectively. The mean annual ETa estimated for the whole estate were 107 Mm<sup>3</sup>, 140 Mm<sup>3</sup>, and 178 Mm<sup>3</sup> using SEBAL, SSEB, and SSEBop, respectively. Even though the algorithms should be validated through field observation, they have potential to be used for effective estimation of ET in the sugarcane estate.

**Keywords:** ET; CWR; landsat ETM+; remote sensing; SEBAL; SSEB; SSEBop

## 1. Introduction

Water is one of the most important limited natural resources crucial for all socio-economic and environmental needs to be managed in a sustainable way to ensure its long-term availability.

Judicious management of precious land and water resources is emerging as one of the biggest challenges of the 21<sup>st</sup> century. Both water and land resources are finite, but competitive demand from other sectors is increasing. Managing water for multiple benefits and between competing demands is occupying the minds of irrigators, catchment water managers and policy-makers. Agriculture is by far the largest water user sector and the goal of every grower is to practice irrigation management to fulfill water needs profitably, safely, and in an environmentally responsible way. Irrigation depends on reliable supplies of fresh, clean water from surface and/or groundwater sources. Knowing how much water moves through soils and crop canopy can help growers use irrigation water more effectively with less risk to water sources.

As stated by Hemukamara *et al.* (2003) and Burdette *et al.* (2015) [1, 2], evapotranspiration (ET) which is a process governed by the energy and heat exchanges at the land surface, with the upper bound being constrained and controlled by the amount of available energy and water respectively is also an important factor for evaluating water productivity and monitoring of irrigation performance. Therefore, an estimation of spatially distributed crop water consumption is challenging, but important to determine water balance at different scales to promote efficient management of water resources. Evapotranspiration from irrigated agriculture is an important issue in arid and semi-arid regions where it has large impact on water resources depletion and water management (Tasumi and Allen, 2007), [3]. Accurate determination of crop ET is essential for designing irrigation systems and for irrigation scheduling. Remote sensing data can resolve difficulties in determining water balance due to scientific developments in the calculation of spatially distributed actual evapotranspiration (Chen *et al.*, 2014; vanino *et al.*, 2015; and Nouri *et al.*, 2013) [4,5,6]. The use of remote sensing techniques to estimate evaporation is achieved by solving the energy balance of thermodynamics fluxes at the surface of the earth and it is used for calculating the actual evapotranspiration (ET<sub>a</sub>) based on the equilibrium between the radiation balance and the energy balance at the surface of the earth.

The main objectives of this study were:

- To estimate actual ET using Surface Energy Balance Algorithm for Land (SEBAL), Simplified Surface Energy Balance (SSEB), Operational Simplified Surface Energy Balance (SSEBop); and Penman-Monteith Methods;
- To compare the actual ET results of SEBAL, SSEBop and SSEB; and
- To calculate the crop water requirement of the sugarcane estate

## 2. Materials and Methods

### 2.1. Description of the Study Area

The Wonji-Shoa Sugarcane Estate lies downstream of the Koka Dam in the Central Rift Valley of Ethiopia in the upper Awash River basin around 114 km from Addis Ababa within the geographical boundaries of 8° 21' to 8° 29' N latitudes and 39° 12' to 39° 18' E longitudes at an altitude of about 1,540 m above sea level (Melaku, 2009) [7]. Currently the estate is cultivating more than 9352 hectare of irrigated land using furrow irrigation system.

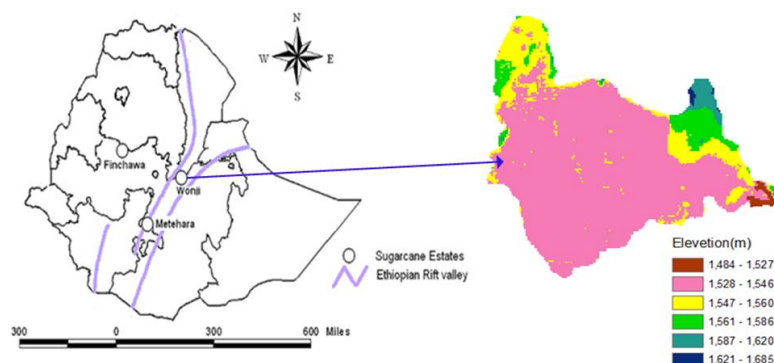


**Figure 1.** Location and topographic map of the study area

In the estate, generally, the topography of the farm is very gentle slopes with flood prone plains of Awash River. The soils of Wonji-Shoa have been described predominantly as a complex of gray, cracking clays in the topographic depressions and semiarid, brown soils. The main crops cultivated are sugarcane, haricot bean and crotalaria. Sugarcane is planted at a rate of 16-18 t/ha in the estate and it is cultivated as perennial monocrop. The mean annual relative humidity ranges from 43.2 to 68.4%. It is described as tropical wet climate with uniform warmth throughout the year and receives an average annual rainfall of 831.2 mm, average daily evapotranspiration of 4.5 mm/day, mean annual maximum and minimum temperatures of 27.6 °C and 15.2 °C, respectively and the average sunshine hour is 9 hours in dry summer and 6.5 hours in August as cited in (Girma and Awulachew, 2007) [8]. At Wonji, in the Upper Valley, the mean annual PET is 1810 mm, over twice the mean annual rainfall (Shimelis, 2004) [9].

2.2 Data Collection and Analysis

2.2.1 Data collection

I. Remote sensing data

The main remote sensing input used for this study is Landsat7 ETM+ data having spatial resolution of 30m for visible and near infrared bands (b1 to b5 and b7) and 60m resolution for thermal band (b61 and b62) at satellite nadir provided by the United States Geological Survey (USGS) Earth Observation System (EOS) Data Gateway.

II. Meteorological data

The Meteorological data in daily time steps were collected from Wonji Shoa sugarcane estate research center weather station during the four satellite overpass dates as shown in table 1 below.

Table 1. Average/ daily weather conditions at the satellite overpass time

Dates	Temperature (°C)	Humidity (%)	Wind speed at 2m (m/sec)	Actual sunshine hour (hour)	Precipitation (mm)	ETo Penman (mm)
Jan 25,2002	17.4	43	3.1	10.5	0.0	5.49
Feb 26,2002	20.5	36	2.8	11	0.0	6.31
Sept 6,2002	21.8	58	1.7	0.0	0.0	3.11
Oct 8,2002	19.4	46	2.4	11	0.0	5.39

III. Software packages used

The main software packages used were Earth Resource Data Analysis System (ERDAS) IMAGINE version10, CROPWAT8, ArcGIS 9.3and Saga software.

2.2.2 Data analysis

I. Image analysis for SEBAL parameter extraction

The original satellite images were properly prepared for use in SEBAL, SSEB and SSEB<sub>op</sub> algorithms and were applied to Landsat-7 ETM+ data for assessing the actual ET by calculating the ET flux for each pixel of the satellite image as a “residual” of the surface energy balance equation. The Landsat ETM+ seven bands were layered inside ERDAS IMAGINE, in order from band 1 to band 7 to create an image file for use in the image analysis process. After that, a smaller subset image was created for Wonji Shoa sugarcane plantation farm. Having estimated the land surface parameters such as NDVI, reflectance, emissivity and temperature, the selected algorithms were employed to

estimate daily actual ET. The first step used in the SEBAL procedure was to compute the net surface radiation flux ( $R_n$ ) using the surface radiation balance equation.

$$R_n = (1 - \alpha)R_{S\downarrow} + R_{L\downarrow} - R_{L\uparrow} - (1 - \varepsilon)R_{L\downarrow} \quad (1)$$

where,  $R_{S\downarrow}$  is incoming shortwave radiation ( $W/m^2$ ),  $\alpha$  is broadband surface albedo (dimensionless),  $R_{L\downarrow}$  is incoming long wave radiation ( $W/m^2$ ),  $R_{L\uparrow}$  is outgoing long wave radiation ( $W/m^2$ ),  $\varepsilon$  is surface thermal emissivity (dimensionless),  $R_n$  represents the actual radiant energy available at the surface. This was accomplished in a series of steps using the ERDAS Model Maker tool to compute the terms in equation(1). The land surface temperature ( $T_s$ ) is computed using the following modified Plank equation and hot and cold pixels were selected.

$$T_s = \frac{K_2}{\ln\left(\frac{\varepsilon \times K_1}{R_c} + 1\right)} \quad (2)$$

where;  $R_c$  is the corrected thermal radiance from the surface using the spectral radiance of band 6,  $\varepsilon$  is the "broad-band" surface emissivity (dimensionless).  $K_1$  and  $K_2$  are constants for Landsat images. The SEBAL process utilizes the "hot" and "cold" pixels to fix boundary conditions for the energy balance. The "cold" pixel is selected as a wet, well-irrigated crop surface having full ground cover by vegetation. The "hot" pixel is selected as a dry, bare agricultural field where ET is assumed to be zero (Bastiaanssen *et al.*, 2002), [10].

Estimation of the Fluxes in the Surface Energy Balance Equation: the second step of the SEBAL procedure is to compute the terms soil heat flux( $G$ ) and sensible heat flux ( $H$ ) of the surface energy budget equation as a function of net radiation flux ( $R_n$ ) as follows:

$$R_n = G + H + \lambda ET \quad (3)$$

where;  $R_n$  is the net radiation at the surface ( $W/m^2$ ),  $G$  is the soil heat flux ( $W/m^2$ ),  $H$  is the sensible heat flux to the air ( $W/m^2$ ), and  $\lambda ET$  is the latent heat flux ( $W/m^2$ ).

This equation is solved through the following steps using the ERDAS Model Maker tool.

Soil Heat Flux ( $G$ ): SEBAL first computes the ratio  $G/R_n$  using the following empirical equation developed by Bastiaanssen (2000), [11] representing values near midday:

$$\frac{G}{R_n} = \frac{(T_s - 273)}{\alpha} (0.0038\alpha + 0.0074\alpha^2)(1 - 0.98 NDVI^4) \quad (4)$$

where;  $T_s$  is the surface temperature ( $^{\circ}C$ ),  $\alpha$  is the surface albedo, and NDVI is the Normalized Difference Vegetation Index.  $G$  is then readily calculated by multiplying  $G/R_n$  by the value for  $R_n$ .

Sensible Heat Flux ( $H$ ): The sensible heat flux ( $H$ ) is computed as follows for heat transport:

$$H = \frac{\rho \times c_p \times dT}{r_{ah}} \quad (5)$$

where;  $\rho$  is air density ( $kg/m^3$ ),  $C_p$  is air specific heat ( $1004 J/kg/K$ ),  $dT$  ( $K$ ) is the temperature difference ( $T_1 - T_2$ ) between two heights ( $z_1$  and  $z_2$ ), and  $r_{ah}$  is the aerodynamic resistance to heat transport ( $m/s$ ). Equation (5) is difficult to solve because there are two unknowns,  $r_{ah}$  and  $dT$ . To facilitate this computation, the two "anchor" pixels (where reliable values for  $H$  can be predicted and a  $dT$  estimated) and the wind speed at a given height were utilized.

Latent Heat Flux ( $\lambda ET$ ), Instantaneous ET ( $ET_{inst}$ ), and Reference ET Fraction ( $ET:F$ ): In SEBAL mode latent heat flux is computed as residual variables of the energy balance equation. It can be computed for each pixel using Equation (5):

$$\lambda ET = R_n - G - H \quad (6)$$

where;  $\lambda ET$  is an instantaneous value for the time of the satellite overpass ( $W/m^2$ ). An instantaneous value of ET in equivalent evaporation depth is computed as:

$$ET_{inst} = 3600 \frac{\lambda ET}{\lambda} \quad (7)$$

where; is the instantaneous ET (mm/hr), 3600 is the time conversion from seconds to hours, and  $\lambda$  is the latent heat of vaporization or the heat absorbed when a kilogram of water evaporates (J/kg). The reference ET Fraction (ET<sub>r</sub>F) is computed using ET<sub>inst</sub> and weather data.

$$ET_rF = \frac{ET_{inst}}{ET_o} \quad (8)$$

where; ET<sub>inst</sub> is from Equation 6 (mm/hr) and ET<sub>o</sub> is the reference ET at the time of the image from the CROPWAT software (mm/hr). ET<sub>r</sub>F is similar to the well-known crop coefficient, K<sub>c</sub> and is used to extrapolate ET from the image time to 24-hour or longer periods.

Daily (24-Hour) Evapotranspiration (ET<sub>24</sub>): SEBAL computes the ET<sub>24</sub> by assuming that the instantaneous ET<sub>r</sub>F computed above is the same as the 24-hour average and ET varies throughout the day while ET<sub>r</sub>F is relatively constant. Finally, the ET<sub>24</sub> (mm/day) can be computed as:

$$ET_{24} = ET_rF \times ET_{o-24} \quad (9)$$

where; ET<sub>o-24</sub> is the cumulative 24-hour ET<sub>o</sub> for the day of the image.

## II. SSEB model overview and parameter estimation

The main concept of the SSEB approach in Senay *et al.* (2011), [12] is the joint use of reference ET and land surface temperature data. The surface energy balance is first solved for a reference crop condition (assuming full vegetation cover and unlimited water supply) using the standardized Penman–Monteith equation (Allen *et al.*, 1998), [13]. ET fractions (ET<sub>f</sub>) account for differences in water availability in the landscape; and are used to adjust the reference ET (ET<sub>o</sub>) based on the land surface temperature (T<sub>s</sub>) of the pixel (Eq. (2) for ET<sub>f</sub>). The ET fraction (ET<sub>f</sub>) is calculated for each pixel “x” by applying Eq. (10) to each of the 4-date Landsat T<sub>s</sub> grids.

$$ET_f = \frac{TH - T_x}{TH - TC} \quad (10)$$

where TH and TC are the average radiometric surface temperature at hot and cold pixels, respectively; and T<sub>x</sub> is the radiometric surface temperature for any given pixel in that image. The basic approach of calculating ET<sub>a</sub> involves only two steps: ET<sub>a</sub> is simply a product of the ET fraction (ET<sub>f</sub>) and ET<sub>o</sub> via Eqs. (11) and (12).

$$ET_a = ET_f \times ET_m \quad (11)$$

where ET<sub>a</sub> is actual ET, ET<sub>f</sub> is ET fraction, and ET<sub>m</sub> is maximum ET for the region. When grass reference ET<sub>o</sub> is calculated from weather data, ET<sub>m</sub> is estimated as:

$$ET_m = \alpha \times ET_o \quad (12)$$

where the multiplier  $\alpha$  is recommended to be 1.2 to estimate ET for tall, full cover crops such as alfalfa, corn, sugarcane and wheat which are aerodynamically rougher than the clipped grass reference and have greater leaf area and thus greater canopy conductance (Allen *et al.*, 1998), [13].

## III. New parameterization approach (SSEB<sub>op</sub>)

The method is developed by Senay *et al.* (2013), [14] and it is based on the Simplified Surface Energy Balance (SSEB) approach which is now parameterized for operational applications, renamed as SSEB<sub>op</sub>. The innovative aspect of the SSEB<sub>op</sub> parameterization is that it uses pre-defined, boundary conditions that are unique to each pixel for the “hot” and “cold” reference conditions. To estimate ET routinely, the only data needed for this method are T<sub>s</sub>, climatology air temperature (T<sub>a</sub>) and ET<sub>o</sub>. With

this simplification, actual ET ( $ET_a$ ) is estimated using equation 13 as a fraction of the  $ET_o$  and the ET fraction ( $ET_f$ ) is calculated using equation 14.

$$ET_a = ET_f \times \alpha ET_o \quad (13)$$

where  $ET_o$  is the grass reference ET;  $\alpha$  is a crop coefficient with a recommended value of 1.2.

$$ET_f = \frac{T_h - T_s}{T_h - T_c} \quad (14)$$

where  $T_s$  is the satellite observed land surface temperature of the pixel whose  $ET_f$  is being evaluated on a given time-period.  $T_h$  is the estimated  $T_s$  at the idealized reference “hot” condition of the pixel, the cold reference value  $T_c$ , is the estimated  $T_s$  at the idealized reference “cold” condition of the pixel of the same time period.

$T_c$  determination:  $T_c$  boundary condition was determined using correction coefficient as :

$$T_c = c \times T_a \quad (15)$$

where  $T_a$  is the climatology near-surface maximum  $T_a$  for the period;  $c$  is a correction factor that relates  $T_a$  to  $T_s$  on a well-watered, fully transpiring vegetation surface. The correction coefficient  $c$  is determined as a seasonal average between  $T_s$  and  $T_a$  on all pixels where NDVI is greater or equal to 0.8. Preliminary results showed that this coefficient vary little from place to place. However, for localized applications, one is advised to develop local specific ‘ $c$ ’ values.

$$c = \frac{T_{scold}}{T_a} \quad (16)$$

where  $T_{scold}$  is the satellite-based  $T_s$  at the cold pixel where  $NDVI > 0.8$  and  $T_a$  is the corresponding air temperature at same location and season. The correction factor for the study area was determined to be 0.989 when both  $T_s$  and  $T_a$  were processed in Kelvin units which is calculated as the spatially averaged values of available locations and is usually obtained in peak-season irrigated areas and forested regions.

Pre-defined  $dT$  and hot boundary condition: Once the  $T_c$  is defined as the fraction of the climatological  $T_a$ , the hot boundary condition ( $T_h$ ) can also be defined by a constant difference ( $dT$ ) that will be added to the  $T_c$  of each pixel on a given time period. Thus, the second key component of this method is estimation of  $dT$  from energy balance principles for a clear sky condition. The pre-defined  $dT$  is solved from the  $R_n$  equation solved for a bare, dry soil where ET is assumed to be zero and sensible heat is assumed maximum (Bastiaanssen, 1998), [15]. Since  $\lambda ET$  and  $G$  are considered 0.0, the magnitude of the radiation balance for a bare, dry soil with the sensible heat equation can be written as follows:

$$R_n = H = p \times c_p \times dT/r_a \quad (17)$$

Since all  $R_n$  is now assumed to be used for sensible heat flux at the hot boundary condition,  $H$  will be approximated by the clear-sky net radiation received at an idealized bare and dry surface for a given pixel on a given period. The next step is to estimate the available clear-sky net radiation that is available for a given period so that  $dT$  can be solved by rearranging Equation 17. After  $R_n$  is estimated for each pixel, the pre-defined  $dT$  was solved using  $R_n$ ,  $c_p$  and  $q$  and  $r_a$  as:

$$dT = \frac{R_n \times r_a}{\rho \times c_p} \quad (18)$$

where  $c_p$  is the specific heat of air at constant pressure ( $1.013 \text{ kJ kg}^{-1} \text{ }^\circ\text{C}^{-1}$ );  $q$  is the density of air which is calculated using Allen *et al.*, 1998 [8];  $r_a$  is the aerodynamic resistance to heat flow from a hypothetical bare and dry surface; it was determined through a quasi-calibration process. Furthermore, comparison with 45 US flux tower ET by Allen *et al.*, 2005, [16] shows that  $110 \text{ ms}^{-1}$  gives a reasonable agreement and decided in this study to fix the  $r_a$  value at  $110 \text{ ms}^{-1}$ .



Therefore, once the expected dT is determined, Th can be calculated as follows:

$$T_h = T_c + dT \tag{19}$$

2.3 Estimating potential evapotranspiration (ET<sub>o</sub>)

The FAO Penman-Monteith method is used as the sole method for determining ET<sub>o</sub> and explicitly incorporates both physiological and aerodynamic parameters.

2.4 Methods of crop evapotranspiration (ET<sub>c</sub>) estimation

ET<sub>c</sub> is calculated by multiplying ET<sub>o</sub> by K<sub>c</sub>, a coefficient expressing the difference in evapotranspiration between the cropped and reference grass surface. In this study the difference were combined into one single coefficient that means the effect of crop transpiration and soil evaporation are combined into a single K<sub>c</sub> coefficient. The Crop water requirements (CWR) were calculated on the basis of monthly effective rainfall (P<sub>eff</sub>) and ET<sub>o</sub>, the first being calculated from average rainfall following the Penman-Monteith approach.

$$ET_c = K_c \times ET_o \tag{20}$$

where ET<sub>c</sub> crop evapotranspiration (mm d<sup>-1</sup>), K<sub>c</sub> crop coefficient (dimensionless), ET<sub>o</sub> reference crop evapotranspiration (mm d<sup>-1</sup>).

3. Results and Discussion

3.1 Relationship of Land Surface Temperature(LST) and NDVI in 2002

Figure 2 below shows the subset images of the study area created using the ERDAS IMAGINE tool with natural (true) color combination of Band 5, Band 4, and Band 3 correspondingly. This helps to distinguish the distribution of NDVI, LST and ET between different land covers and land features. The figures show Awash River and water storage reservoirs marked with blue color, the sugarcane estate covered by sugarcane crop is marked by dark green color, uncultivated irrigated wet fields are seen as black color and bare agricultural areas are marked by light pink color (figure 2).

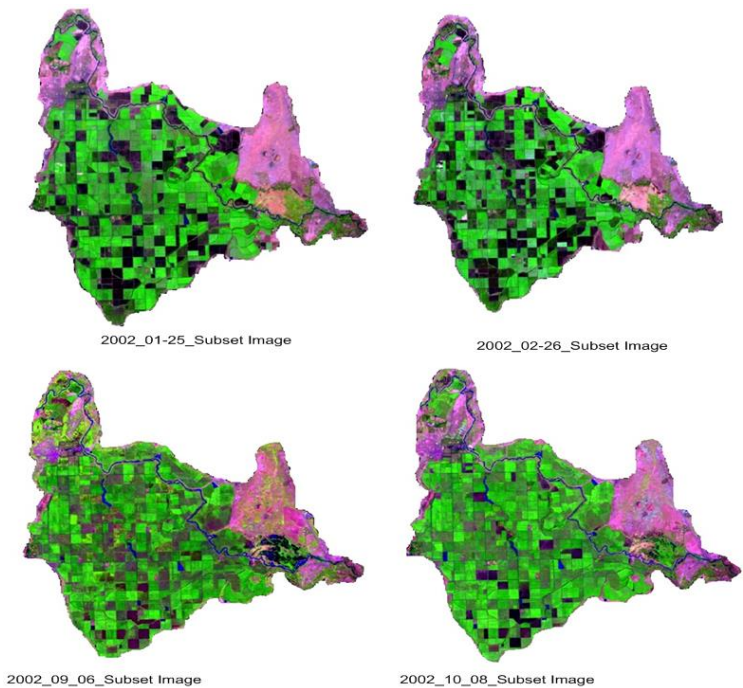


Figure 2. Land cover and features subset images of Wonji Shewa sugarcane estate

The main purpose of this comparison was to show the spatiotemporal variability of land surface temperature which varies with the available moisture on the sugarcane farms, water bodies and vegetation surfaces and it was found to be strongly dependent on the season and moisture availability. Most of the agricultural fields covered by sugarcane plantation and the water storage reservoirs exhibit lower land surface temperature than bare agricultural fields in all images generated and the influence of moisture status was also clearly noted. The images from the predominantly hotter and drier pixels contrast well with the generally cooler and wetter surface covers. There is good linear relationship between NDVI and LST with an  $r^2$  value of Jan, Feb, Sept, and Oct images of 0.72, 0.704, 0.38, and 0.60, respectively (table 2).

**Table 2.** Mean daily temperature and NDVI values of selected days in 2002.

Parameters	Statistics	Image dates			
		Jan	Feb	Sept	Oct
LST(K)	Minimum	291	297	297	296
	Maximum	313	325	319	324
	Mean	300	310	304	306
	Standard deviation	4.49	5.89	3.73	4.97
NDVI	Minimum	-0.33	-0.37	-0.23	-0.25
	Maximum	0.77	0.765	0.86	0.81
	Mean	0.314	0.305	0.42	0.37
	Standard deviation	0.16	0.15	0.21	0.20

3.2 Spatial and Temporal Distribution of Evapotranspiration

The spatial and temporal variability in the actual evapotranspiration estimated using the SEBAL, SSEB, and SSEB<sub>op</sub> algorithms are presented and discussed in the following subsections. The satellite image had relatively good resolution(30m by 30m) which make the results more acceptable and in a good agreement with observed ET<sub>a</sub> values as indicated by the study findings of Nouri *et al.* (2016), [17].

3.2.1 Spatial distribution of ET<sub>a</sub> during January, 2002

The estimated daily minimum and maximum ET<sub>a</sub> values in January using SEBAL, SSEB and SSEB<sub>op</sub> algorithms were 0.0 and 6.85, 0.0 and 6.78, and 0.05 and 8.25 mm/day respectively with mean and standard deviation values of 2.88 and 1.41, 3.45 and 1.66, and 4.88 and 1.68 respectively (figure 3). Comparative assessment of standard deviation of ET<sub>a</sub> over the sugarcane plantation indicated moderate spatial variability of ET<sub>a</sub> due to soil moisture variability which itself is dependent on irrigation application and rainfall availability. Dry periods exhibit greater variability than wetter periods. The SEBAL algorithm ET<sub>a</sub> estimation on well irrigated moist sugarcane fields, water storage reservoirs including Awash River was higher than the other cultivated sugarcane plantation fields. It also showed that no moisture was lost by ET in most of bare agricultural fields. SSEB and SSEB<sub>op</sub> ET<sub>a</sub> estimation over moist and cultivated sugarcane fields looked consistent and good. The ET over some bare agricultural fields especially SSEB<sub>op</sub> contradicted SEBAL results. All the three algorithm results showed that moist surfaces have higher ET<sub>a</sub> values. Moreover, dry agricultural fields exhibits generally lower ET<sub>a</sub> values. This shows that the remote sensing technique can capture the spatial variability of ET<sub>a</sub> . The highest mean ET<sub>a</sub> values in the well watered sugarcane fields resulted due to mid-season stage crop developed through irrigation and in swamp of the plain and night water storage reservoirs. Generally higher residual ET<sub>a</sub> values were observed over well grown sugarcane fields and water storage areas and lower values were observed over dry agricultural fields. The Root



Mean Square Error (RMSE) values between SSEB and SEBAL, SSEB<sub>op</sub> and SEBAL, and SSEB and SSEB<sub>op</sub> ET<sub>a</sub> estimates were 0.548, 0.548, and 0.99 respectively.

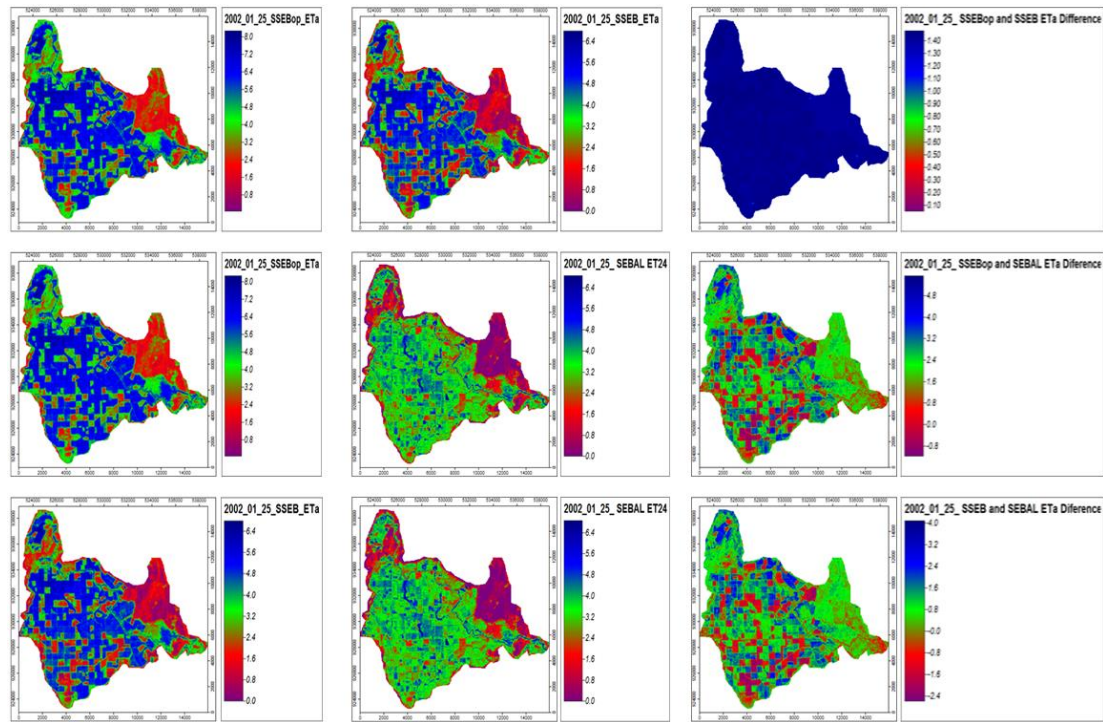


**Figure 3.** January 25, 2002 actual evapotranspiration (mm/day) at Wonji sugarcane estate

3.2.2 Spatial distribution of ET<sub>a</sub> during February 26, 2002

The daily minimum and maximum ET<sub>a</sub> values of February 26, 2002 using SEBAL, SSEB and SSEB<sub>op</sub> algorithms were found to be between 0.0 and 9.36, 0.0 and 7.81, and 0.0 and 8.82 mm/day, respectively (figure 4). All the three algorithms ET<sub>a</sub> estimates on well irrigated and moist sugarcane fields, water storage reservoirs including Awash River were higher than the uncultivated sugarcane plantation fields and bare agricultural fields. In summary, it was noted that SSEB<sub>op</sub> and SSEB ET<sub>a</sub> estimates were closer and consistent over fully covered and well grown sugarcane fields, and also were higher than SEBAL ET<sub>a</sub> estimates. The SEBAL algorithm ET<sub>a</sub> estimates over water storage areas were higher than SSEB<sub>op</sub> and SSEB ET<sub>a</sub> estimates. On the contrary, SEBAL ET<sub>a</sub> estimates over uncultivated sugarcane fields were observed to be higher than SSEB<sub>op</sub> and SSEB ET<sub>a</sub> estimates. Over dry agricultural fields, the ET<sub>a</sub> estimates of all the three algorithms were close to each other. The Root Mean Square Error (RMSE) values of 0.739 between SSEB and SEBAL, 0.753 between SSEB<sub>op</sub> and SEBAL, and 0.994 between SSEB and SSEB<sub>op</sub> ET<sub>a</sub> were observed.

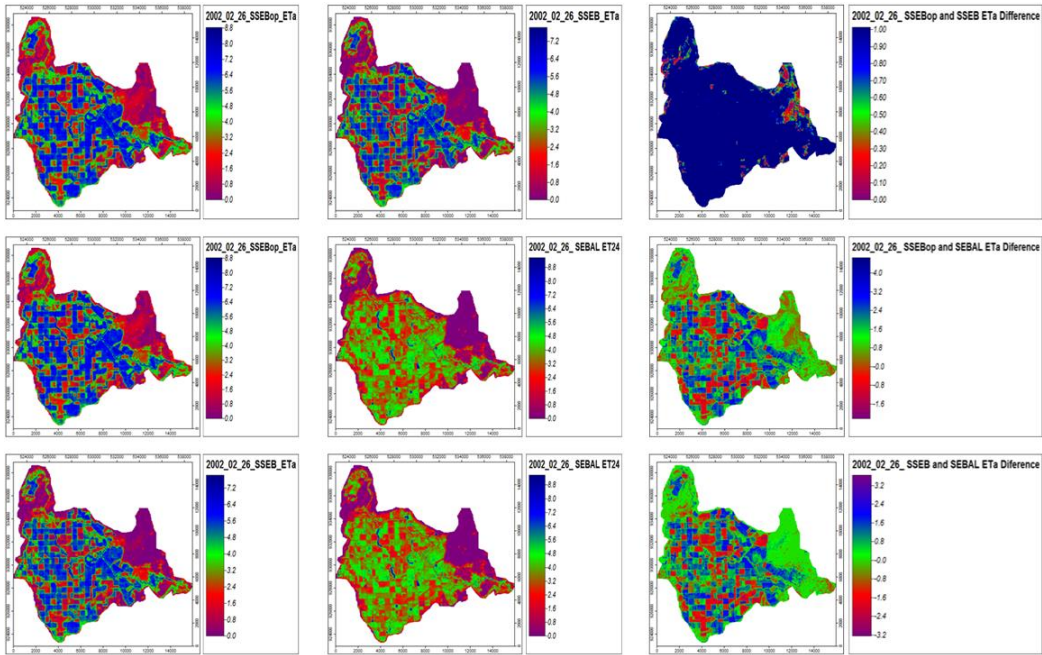


**Figure 4.** February 26, 2002 actual evapotranspiration (mm/day) at Wonji sugar estate

3.2.3 Spatial distribution of ET<sub>a</sub> during September 06, 2002

The September 06, 2002 minimum and maximum daily ET<sub>a</sub> values were 0.0 and 3.61 mm/day for SEBAL, 0.0 and 3.65 mm/day for SSEB and 0.2 and 4.0 mm/day for SSEB<sub>op</sub> algorithms (figure 5). All the three algorithms ET<sub>a</sub> estimates on well grown and moist sugarcane fields, night storage reservoirs and on the Awash River were higher than other dry agricultural fields. The comparisons with earlier months showed that more water was lost by ET<sub>a</sub> on bare agricultural (uncultivated) fields. This is expected as September is end of the rainy month and the soil should contain more moisture for subsequent ET, but generally all of the three algorithms ET<sub>a</sub> estimates were lower due to higher humidity and a decreased solar radiation associated with the effect cloud cover at the satellite overpass time. During September, the optimum climatic condition to satisfy the evaporative demand of the area were higher than the other months except the cloud cover which resulted in lower ET<sub>a</sub> values throughout the sugarcane estate. The standard deviation of ET<sub>a</sub> over the sugarcane plantation were also lower indicating lower spatial variability of ET<sub>a</sub> due to less soil moisture variability. Even though the soil was saturated due to excess summer rainfall providing the opportunity for ample evapotranspiration in the area, lower atmospheric demand (low radiant energy of the sun) due to cloud cover and higher humidity causes the entire sugarcane estate to have lower ET<sub>a</sub> values. ET<sub>a</sub> estimate for SSEB<sub>op</sub>, SSEB and SEBAL during September were close to each other and looked consistent and higher over the entire sugarcane estate. The Root Mean Square Error (RMSE) values were 0.847 for SSEB and SEBAL, 0.846 for SSEB<sub>op</sub>, and SEBAL, and 0.999 for SSEB and SSEB<sub>op</sub> ET<sub>a</sub> estimates.

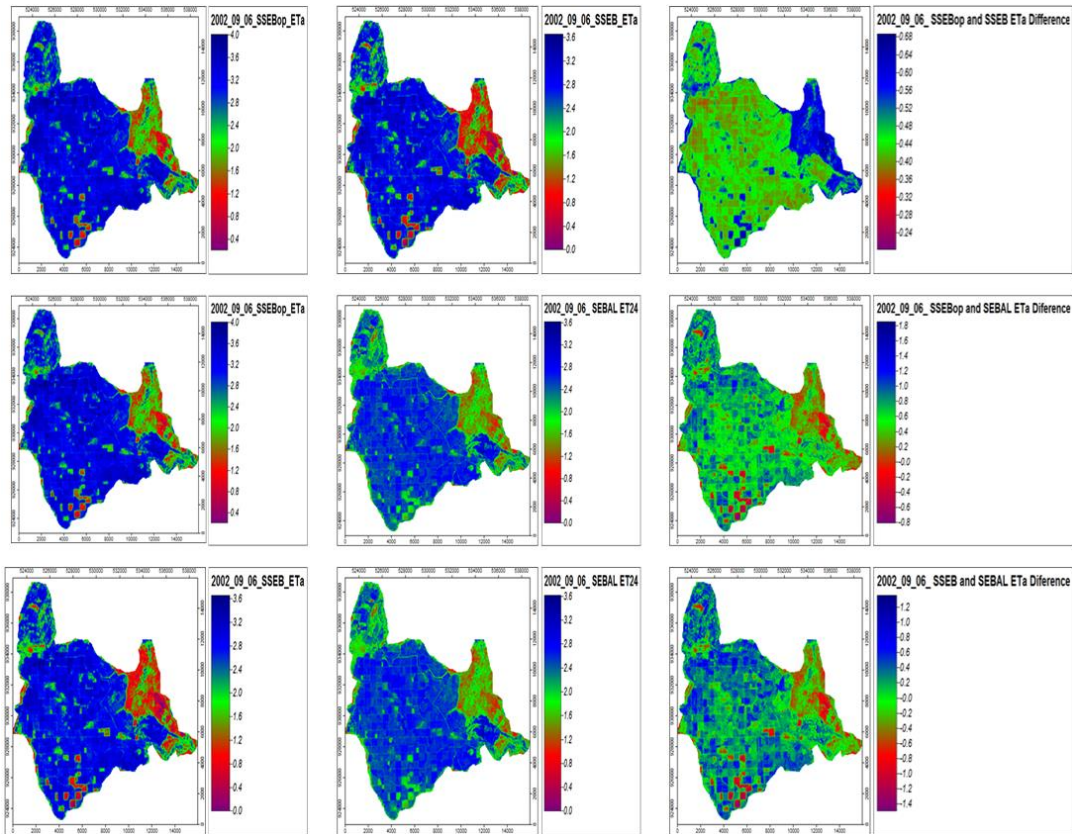


Figure 5. September 6, 2002 actual evapotranspiration (mm/day) at Wonji sugar estate

3.2.4 Spatial distribution of ET<sub>a</sub> during October 8, 2002

The estimated daily minimum and maximum ET<sub>a</sub> values on October 8, 2002 using SEBAL, SSEB and SSEB<sub>op</sub> algorithms were 0.0 and 6.83, 0.0 and 6.46, and 0.0 and 7.4 mm/day, respectively (figure 6). The corresponding mean and standard deviation values respectively were 1.57 and 1.08 for SEBAL, 3.62 and 1.46 for SSEB, and 4.18 and 1.65 for SSEB<sub>op</sub>. The ET<sub>a</sub> values obtained on bare agricultural fields suggested that there were still adequate residual moisture from the preceding rainy months contributing to the overall ET. All the three algorithm results consistently exhibited that moist surfaces have higher ET<sub>a</sub> values as compared to dry agricultural fields. During October 2002, the optimum climatic condition to satisfy the evaporative demand of the area were higher and the standard deviation of ET<sub>a</sub> over the sugarcane plantation were lower indicating lower spatial variability of ET<sub>a</sub> in relation to the soil moisture variability. Generally higher residual values are observed over well grown sugarcane fields and night storage areas, and lower values were observed over dry agricultural fields. The residual difference of ET<sub>a</sub> estimates between SSEB<sub>op</sub> and SSEB varied from 0.4 – 0.94 on moist sugarcane fields, and 0.0 – 0.39 mm/day over dry agricultural lands. The ranges of the residual difference of ET<sub>a</sub> estimates between SSEB<sub>op</sub> and SEBAL were -1.29 – 5.98 mm/day, between SSEB and SEBAL were from -1.7 – 5.2 mm/day. The Root Mean Square Error (RMSE) value between SSEB and SEBAL, SSEB<sub>op</sub> and SEBAL, and SSEB and SSEB<sub>op</sub> ET<sub>a</sub> estimation were 0.573, 0.573, and 1.00, respectively.



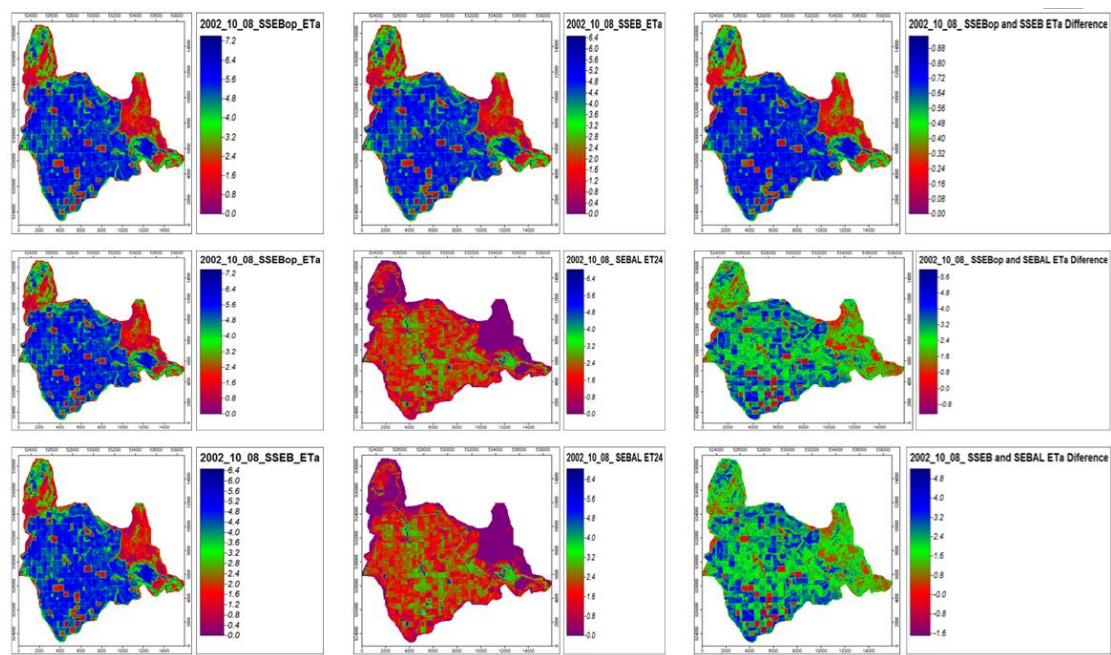


Figure 6. October 8, 2002 daily evapotranspiration (mm/day) at Wonji sugar estate

3.4 Crop and Irrigation Water Requirement (CWR)

As shown in Table 3 below, estimates of the average annual water consumption by SSEB<sub>op</sub> were 40 % higher than SEBAL and 21% higher than SSEB. The mean annual ET<sub>a</sub> estimated for the whole estate were 107 Mm<sup>3</sup>, 140 Mm<sup>3</sup>, and 178 Mm<sup>3</sup> using SEBAL, SSEB and SSEB<sub>op</sub> , respectively (table 3) and the mean annual PET was 219Mm<sup>3</sup>.

Table 3. Monthly and annual average actual ET for Wonji Shoa sugar cane Estate using different algorithms

Month	Monthly Average Estates Consumptive Water Use (Mm <sup>3</sup> )							
	SSEBAL		SSEB		SSEB <sub>op</sub>		MOD16	
	mm/day	mm/month	mm/day	mm/month	mm/day	mm/month	mm/day	mm/month
Jan	2.88	11	3.45	13	4.88	18	1.23	5
Feb	2.82	10	3.01	11	3.95	15	1.26	5
Sept	2.31	8	2.46	9	2.92	11	2.66	10
Oct	1.57	6	3.62	13	4.18	15	1.99	7
Annual Estates Consumptive Use Estimates (Mm <sup>3</sup> )								
Average	2.39	107	3.14	140	3.98	178	1.79	80

The required timing and amount of applied water for the sugarcane were calculated based upon the prevailing climatic conditions, growing season, growing and harvesting date, root depth, and allowable depletion, soil physical properties, availability of water resources, field water losses and useful rainfall and therefore the CWR and irrigation water requirement (IR) of sugarcane crop were computed by considering the field water balance in the crop root zone. The total CWR, IR and effective rain for January and March planted sugarcane were estimated to be 2468.8, 2061.6 and 423.8 mm/yr and 2281.9, 1851.0 and 437.8 mm/yr respectively.

4. Conclusions

In this research, ET estimates were made using SSEB<sub>op</sub>, SSEB, and SEBAL algorithms for the Wonji Shoa Sugarcane Estate. Landsat7 ETM+ images of four days in 2002, (i.e. January 25, February, 26, September 6 and October, 8 2002), were used and the actual ET was computed using the three algorithms. The result of this study generally demonstrates that these three algorithms could be used to provide vital information on evaporative loss and moisture condition of the sugarcane estate. It can be considered as operational and feasible methods to predict actual ET and to improve water management and modeling processes in the sugarcane estate. The major findings of the study clearly showed that remote sensing can have a tremendous potential for estimating evapotranspiration and water management at farm and basin level. The simple averaged annual actual evapotranspiration by SEBAL, SSEB and SSEB<sub>op</sub> showed that the estate losses 107, 140, 178, and 80 Mm<sup>3</sup> of water per year, respectively due to ET and these values are closer to actual evaporation need to be substantiated through field measurement. The analysis of actual ET in the sugarcane estate estimated by remote sensing method revealed large spatial and temporal variability which closely followed the variability in soil moisture and land use characteristics which otherwise would have been difficult to get it using the indirect methods and the evaporative fraction (parameter determines energy partitioning) in the sugarcane estate, exhibits similar regional distribution patterns as evaporation rate in the sugarcane estate. The integration of remote sensing techniques and distributed hydrological models can produce better results.

**Acknowledgement:** The study was supported by the United States Agency for International Development (USAID) under the Africa-US Higher Education Initiative - HED052-9740-ETH-11-01. The authors wishes to express his gratitude for the opportunity. I am greatly indebted to my advisors Dr. Tena Alamirew, Dr. Gabriel Senay, and Dr. Mekonnen G/ Michael for their guidance and valuable comments from the preparation of the concept until the compilation of this thesis. I also thank Prof. Junming Wang for his useful comments during the thesis preparation. I thankfully acknowledge Ethiopian Institute of Water Resources (EIWR) community and Arba Minch University for all the support I have been enjoying. I would like to express my sincere gratitude to Wonji Research and Training Center community for the support during field work. The Landsat ETM+ data were obtained from the NASA Land Processes Distributed Active Archive Center (LP DAAC), USGS/ Earth Resources Observation and Science (EROS) Center.

## References

- [1] H. Hemakumara, L. Chandrapala, and F. Moene, "Evapotranspiration fluxes over mixed vegetation areas measured from large aperture scintillometer," *Journal of Agricultural Water Management*, Vol.58, pp. 109-122, 2003.
- [2] J. Burdette, N. Christopher, and D. Heeren, "Evaluation of a hybrid remote sensing evapotranspiration model for variable rate irrigation management," *Biological Systems Engineering: Papers and Publications*. Paper 380, 2015.
- [3] M. Tasumi, and R. Allen, "Satellite-based ET mapping to assess variation in ET with timing of crop development," *Journal of Agricultural Water Managment*, Vol.8, pp. 54-62, 2007.
- [4] Y.Chen, J.Xia, S.Liang, J.Feng, J.Fisher, L.Xin, X.Li, S.Liu, Z.Mad, A.Miyata, Q.Mu, L.Sun, J.Tang, K.Wang, J.Wen, Y.Xue, G.Yu, T.Zha, L.Zhang, Q.Zhang, T.Zhao, L.Zhao, and W.Yuan, "Comparison of satellitbased evapotranspiration models over terrestrial ecosystems in China," *Remote Sensing of Environment*, 140, 279-293, 2014.
- [5] S. Vanino, G. Pulighe, P. Nino, C. Michele, S. Falanga and G. D'Urso, "Estimation of evapotranspiration and crop coefficients of Tendone Vineyards using multi-sensor remote sensing data in a Mediterranean environment," *Journal of Remote Sensing*, Vol. 7, pp. 14708-14730, 2015.
- [6] H. Nouri, S. Beecham, F. Kazemi, A. Hassanli, and S. Anderson, "Remote sensing techniques for predicting evapotranspiration from mixed vegetated surfaces," *Hydrology and Earth System Sciences*, Vol. 10, 3897-3925, 2013.
- [7] G. Melaku, "The impact of snail control on the prevalence and intensity of schistosomiasis mansoni in Finchaa and Wonjishoa sugar estates:Post-pilot control analysis," MSc thesis, Addis Ababa University, pp. 1-74, 2009.
- [8] M. Girma, and B. Awulachew, "Irrigation Practices in Ethiopia:Characteristics of Selected Irrigation Schemes," *Working Paper Vol.124*, pp. 1-84, 2007.



- [9] B. Shimelis, "Stream flow simulation for the upper upper Awash basin," MSc. thesis, Addis Ababa university, pp. 7, 2004.
- [10] W. Bastiaanssen, M. Ud-din-Ahmed, and Y. Chemin, "Satellite surveillance of evaporative depletion across the Indus Basin," *Journal of Water Resources*, vol. 38 (12), pp. 1273–1282, 2002.
- [11] W. Bastiaanssen, "SEBAL-based sensible and latent heat fluxes in the irrigated Gediz Basin, Turkey," *Journal of Hydrology*, vol. 229, pp. 87–100, 2000.
- [12] G. Senay, M. Budde, J. Verdin, "Enhancing the Simplified Surface Energy Balance (SSEB) approach for estimating landscape ET: Validation with the METRIC model," *Agricultural Water Management*, vol. 98, pp. 606–618, 2011.
- [13] R. Allen, L. Pereira, D. Raes, and M. Smith, "Crop evapotranspiration: guidelines for computing crop water requirements in United Nations FAO, Irrigation and Drainage Paper 56, FAO, Rome, Italy," 1998.
- [14] G. Senay, S. Bohms, R. Singh, P. Gowda, N. Velpuri, H. Alemu and J. Verdin, "Operational evapotranspiration mapping using remote sensing and weather datasets: a new parameterization for the SSEB approach," *Journal of American Water Resources Research*, In Press, 2013.
- [15] W. Bastiaanssen, M. Menenti, M. Feddes, and R. Holtslag, "A remote sensing surface energy balance algorithm for land (SEBAL): 1) formulation," *Journal of Hydrology*, vol. 212(213), pp. 213–229, 1998.
- [16] R. Allen, M. Tasurmi, A. Morse, and R. Trezza, "A Landsat-based Energy Balance and Evapotranspiration Model in Western US Water Rights Regulation and Planning," *Journal of Irrigation and Drainage Systems*, vol. 19 (3-4), pp. 251–268, 2005.
- [17] H. Nouri, E. Glenn, S. Beecham, S. Chavoshi, P. Sutton, S. Alaghmand, B. Noori, and P. Nagler, "comparing three approaches of evapotranspiration estimation in mixed urban vegetation: field-based, remote sensing-based and observational-based methods," *Journal of Remote Sensing*, Vol. 8, 492, 2016.



© 2016 by the authors; licensee *Preprints*, Basel, Switzerland. This article is an open access article distributed under the terms and conditions of the Creative Commons by Attribution (CC-BY) license (<http://creativecommons.org/licenses/by/4.0/>).